ELSEVIER

Catalysis Today 83 (2003) 59–69

CATALYSIS TODAY

www.elsevier.com/locate/cattod

Flow reversal reactor for the catalytic combustion of lean methane mixtures

S. Salomons [a], R.E. Hayes [a,*], M. Poirier [b], H. Sapoundjiev [b]

[a] *Department of Chemical and Materials Engineering, University of Alberta, 530 Chemical Materials Engineering Building, Edmonton, Alta., Canada T6G 2G6*

[b] *Natural Resources Canada, CANMET/EDRL, 1615 Lionel-Boulet Blvd., P.O. Box 4800, Varennes, Que., Canada J3X 1S6*

Received 1 May 2002; received in revised form 24 October 2002; accepted 18 March 2003

Abstract

This paper describes an experimental investigation of a pilot scale reverse flow reactor for the catalytic destruction of lean mixtures of methane in air. It was found that using reverse flow it was possible maintain elevated reactor temperatures which were capable of achieving high methane conversion of methane in air streams at methane concentrations as low as 0.19% by volume. The space velocity, cycle time and feed concentration are all important parameters that govern the operation of the reactor. Control of these parameters is important to prevent the trapping of the thermal energy within the catalyst bed, which can limit the amount of energy that can be usefully extracted from the reactor.

Keywords: Catalytic combustion; Methane; Reverse flow

1. Introduction

Climate change induced by global warming is a major issue in the world today. It has been suggested that excessive levels of greenhouse gas (GHG) in the atmosphere contribute to global warming via the so-called greenhouse effect. GHG include carbon dioxide, methane and other hydrocarbons, oxides of nitrogen, among others. For reference purposes, GHG emissions are usually reported in terms of equivalent carbon dioxide emissions, and methane has a global warming potential 23 times that of carbon dioxide. Therefore, although the complete combustion of methane produces carbon dioxide in a 1:1 molar ratio, the complete combustion of methane will reduce equivalent carbon dioxide emissions by a factor of about 10.

Typical sources of methane emissions include leaks in gas transmission facilities such as pipelines and compressor stations, upstream oil and gas production facilities, and coal beds. For the latter source, this methane represents a hazard when the coal is mined in an underground mine and must be removed to ensure worker safety. Lean methane commonly present in mine atmosphere may become very dangerous when it accumulates up to the lower explosive limit of 5% by volume [1], especially if mixed with coal dust. Ensuring that mine shaft methane levels are at safe levels is critical to worker safety. As methane is present in the ground and released by mining activities, the methane must be vented and the mine atmosphere cleaned and refreshed.

* Corresponding author. Tel.: +1-780-492-3571; fax: +1-780-492-2881.
E-mail address: bob.hayes@ualberta.ca (R.E. Hayes).

0920-5861/$ – see front matter © 2003 Elsevier B.V. All rights reserved.
doi:10.1016/S0920-5861(03)00216-5

Although the elimination of fugitive methane emissions is beneficial for both safety and climate change reasons, there is an additional motivation for developing methods for capturing and burning fugitive emissions. These emissions are a source of wasted energy which, if captured, can be used as a fuel to provide energy for certain applications. Even lean methane may be burned to produce a utility heat source.

The combustion of fugitive emissions, in particular lean methane emissions, presents some problems. Relatively high concentrations of fugitive emissions can be burnt in a flare using homogeneous combustion. However, the methane concentration in vent gas from coal mines, and in many fugitive emission streams, is typically very low (0.3–1.0% by volume). Homogeneous combustion reactions are unfavourable at such concentrations. Catalytic combustion is therefore a viable alternative to homogeneous reaction, and has been shown to be effective at low methane concentrations [1].

Many catalysts have been used for the combustion of methane, with platinum [2] and palladium [3–7] being the most common, although the use of perovskites has also been reported [8,9]. Homogeneous combustion may also occur in catalytic combustion systems, however, its reaction rate is much lower than the heterogeneous process. At relatively low temperatures (below 1000 °C) and short residence times, homogeneous combustion is usually insignificant compared to the heterogeneous reaction.

To be effective, the reactor must achieve auto-thermal operation, defined as the point at which the energy generated by the combustion reaction is sufficient to maintain essentially complete conversion. Methane is the most difficult of the hydrocarbons to react and therefore requires a relatively high reaction temperature. Unfortunately, fugitive emission streams of lean methane are typically available at ambient temperatures, where the catalytic reaction is very slow, and consequently auto-thermal operation is difficult to attain without pre-heating the feed. In many cases feed pre-heat is not a viable option, and other methods of achieving a sufficiently high reactor temperature must be explored.

A concept that has been successfully exploited in some applications is the catalytic flow reversal reactor (CFRR). The reverse flow concept was first discussed by Frank-Kamenetski [10] and has recently been reviewed by Matros and Bunimovich [11]. In a reversing flow reactor, the feed is periodically switched between the two ends of the reactor using control valves, see Fig. 1 for an illustration of the concept. In Fig. 1(a), the control valves 1 and 4 are opened and the feed flows to the reactor from left to right (forward flow mode). In Fig. 1(b), the control valves 2 and 3 are opened and the feed flows to the reactor from right to left (reverse flow mode). The total cycle consists of these two operations, and the term switch time is used to denote the time at which the flow is changed from forward flow to reverse flow. If the forward and reverse flow times are the same the operation is called symmetric reverse flow operation. If the two flow modes have different times, then the operating mode is called asymmetric operation. The sum of the times for forward and reverse flow is the cycle duration [12].

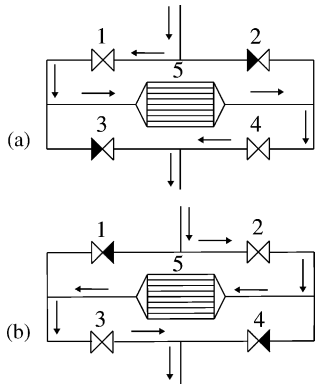

Fig. 1. Illustration of the reverse flow reactor concept.

For an exothermic reaction, the CFRR exhibits a heat trap effect. This effect can be used to achieve and maintain an enhanced reactor temperature compared to a single direction flow mode of operation. The principle of the heat trap effect is illustrated in Fig. 2. Fig. 2(a) illustrates a reactor temperature profile that might be observed in a standard unidirectional flow operation for a combustion reaction. The temperature initially rises slowly as the reaction commences, and then more sharply as the heat liberated in the reaction accelerates the rate owing to the exponential temperature dependence of the rate constant. The shape of the curve depends on the operating conditions, especially the inlet gas temperature. If the inlet temperature is lowered, the reaction rate will fall, and the temperature peak will tend to migrate towards the reactor exit. At

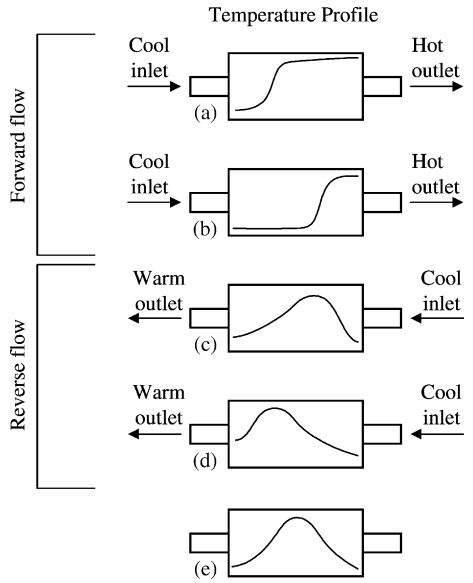

Fig. 2. Illustration of the heat trap effect for reverse flow operation.

a sufficiently low temperature, the reaction will effectively be extinguished and the reactor will lose most of its effectiveness as the leading edge of the "hot spot" (where most of the reaction occurs) migrates out of the reactor. If a temperature pattern shown in Fig. 2(a) or (b) is established, the reverse flow operation can then be used to take advantage of the high temperatures near the reactor exit to pre-heat the reactor feed. When the feed is switched to the "exit", the energy stored in the reactor during the previous reaction is then effectively used to pre-heat the feed. Because this stored energy is added to the feed stream, it is possible to achieve temperatures higher than the adiabatic temperature rise based on the fresh feed inlet temperature. Provided that the reactor is initially at a sufficiently high temperature (which may require some auxiliary heat source) and the cycle duration is carefully chosen, it is possible to achieve auto-thermal reactor operation at feed temperatures well below those required for auto-thermal operation with unidirectional flow. In such a case, a quasi-steady state operation may be achieved in which the reactor temperature profile has a maximum value near the centre of the reactor, which slowly oscillates as the feed is switched between the two ends of the reactor, as shown in Fig. 2(c)–(e). This temperature effect has been called a heat sink [11] and a heat trap [13]. Hanamura et al. [14] demonstrated a reverse flow operation in which the solid phase temperature rise was as high as 13 times the adiabatic temperature rise.

With reverse flow, reactions that are not normally auto-thermal may be run and sustained at lower inlet temperatures and higher conversions than possible in a direct flow adiabatic reactor. A reverse flow reactor may need some pre-heating to bring the catalyst to an acceptable temperature, but a well-designed reactor should be able to sustain itself once running. Liu [15] demonstrated the effectiveness of a CFRR for lean methane combustion in an automobile application, the combustion of excess methane emissions from a natural gas/diesel dual fuel engine. The use of periodic flow reversal in a packed bed reactor for catalytic decontamination of waste gases was also reported by Grozev and Sapoundjiev [16] to achieve conversions of 99.5%. In that work, a heat exchanger was added in the centre of the reactor to remove heat. This ensured that the reactor did not overheat and deactivate the catalyst or damage the reactor. The heat removed from the reactor may be used for tasks such as heating a building or driving a small turbine.

This paper reports on an experimental investigation of a pilot scale reverse flow reactor for the combustion of lean methane mixtures. The effects of cycle time, methane concentration and space velocity are illustrated.

2. Experimental reactor

A schematic of the reactor used in these investigations is given in Fig. 3. The reactor consisted of two parallel sections mounted side by side and connected by a U-bend at the bottom. The reaction sections had an internal diameter of 0.2 m. The two reactor sections are referred to as the left and right sides, respectively. Two three-way valves and associated transfer piping allowed for either forward or reverse flow operating modes. For reference purposes, when the gas flow was from the right section to the left section the mode was referred to as forward flow, whilst flow from left to right was referred to as reverse flow. A thick insulation jacket surrounded the reactors to minimise energy losses to the atmosphere. The reactor system was constructed from Hastelloy which allowed operation at temperatures exceeding 1000 °C.

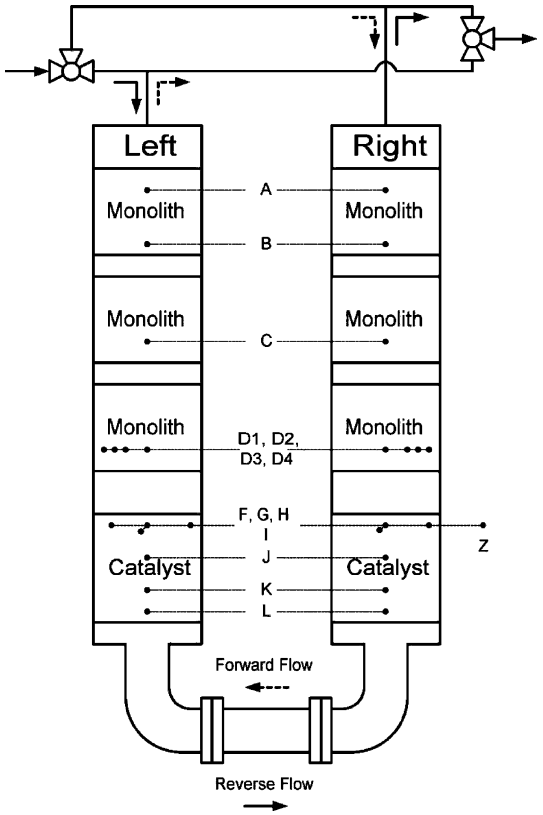

Fig. 3. Reactor schematic showing location of thermocouples and internal sections.

The reactor internals consisted of a combination of open spaces, inert sections, and catalyst sections. In the experiments here, the inert sections were ceramic monoliths, and the active catalyst sections were packed beds of Raschig rings.

Referring to Fig. 3, it is seen that, regardless of flow direction, the incoming gas stream first encountered a sequence of three inert monolith sections, each 0.2 m in height and separated by approximately 2.5 cm, to give a total inert monolith height of 0.65 m. The role of the inert monolith sections was to trap the thermal energy in the reactor. The monoliths were supplied by Corning Incorporated and were composed of Celcor 9475 (EX-20) Cordierite with 33% porosity to give a density of 1683 kg/m^3. The monoliths had 100 cells per square inch (CPSI) with a fractional open frontal area of 0.689. The hydraulic diameter of each cell was 2.16 mm.

The catalyst sections were packed beds of Raschig rings. The metal oxide catalyst was contained on an alumina support prepared by co-precipitation methods. The catalyst is expected to be evenly distributed throughout the solid material.

Atmospheric air was supplied to the reactor via a compressor, the flowrate of which was measured using a mass flowrate meter positioned before the first three-way valve. The methane gas was fed from standard gas bottles of either 99 or 92% methane supplied by BOC Gases.

To initiate reaction it was necessary to pre-heat the catalyst bed. Pre-heating was accomplished through the use of an electric pre-heater blanket on the right side reactor section. This heater was used to bring the active catalyst on the right side of the reactor from ambient temperature to about 500 °C, measured at the electric blanket. Once the right reactor side was pre-heated, the system was operated with inlet flow to the right side (forward flow mode), to push as much thermal energy over to the left side. This method ensured that the reaction occurred in both active sections, and that the left side made significant kinetic contributions to the system.

The reactor could be run in either a fixed direction or in a reversing flow mode. When the reactor is in reversing mode, the valves were used to switch the direction of flow. The operator may determine the length of half cycles in either direction.

3. Data acquisition and control system

A computer-based system provided for reactor control and measurement of gas flowrate, temperatures and concentrations in the reactor. This system used a custom software package that recorded all sensor values at a user-specified interval, generally 5 s. Data were saved in a text file format.

The three-way switching valves that controlled the flow direction were powered by compressed air, and controlled from the computer. Atmospheric pressure was measured using a barometer located next to the reactor.

Gas chromatograph analysis was performed on a number of experiments to measure methane concentration in the reactor. Three GC sampling points were built into the reactor system. There was a GC sampling

point at the present in the mid-section and one sample point near each valve (one before the inlet valve and one after the outlet valve).

Thermal profiles from the reactor system were obtained using 33 thermocouples. Sixteen thermocouples are placed along the centreline of the reactor internals, 12 were placed to obtain radial profiles in the monolith and packed bed sections, and the remaining thermocouples reported temperatures in the insulation, inlet, and outlet. In the thermocouple names, left and right refer to which half of the reactor system contained the relevant thermocouple. Centreline thermocouples in the monolith section (denoted A, B, C and D1 for each of the two sides) were inserted from the top of the reactor down the central monolith channel. A radial profile of the monolith section closest to the catalyst bed was made using thermocouples D1 (closest to the centreline), D2, D3 and D4 (closest to the wall) for each side of the system. Each of these thermocouples occupied a monolith channel. Although these thermocouples blocked a monolith channel, their effect on the heat and mass transport in the reactor is not assumed to be significant because there were approximately 5000 channels in each monolith section. However, the effect of axial conduction on recorded temperatures along the central insert is not known. Rankin et al. [17] discussed potential errors that may be caused by probe wall conduction and the thermal mass of an axial temperature probe. If axial conduction were significant here, the increased thermal energy transfer between thermocouples would lower the highest recorded temperature on the insert (usually D1).

In the packed bed section, thermocouples were inserted from the side, through the insulation and reactor wall. For the centreline thermocouples, the tip of the insert is in the centre of the packed bed. For the radial gradient thermocouples, a single insert is used, with several thermocouples located along the insert. A radial profile of the catalyst on the left side was taken using thermocouples F, G, H and I. Thermocouple G was in the centreline. Thermocouples F, H and I were all 9 cm from the centre of the reactor, except they are in different angular positions. Thermocouples F, G and H were aligned, and thermocouple I was displaced by 90°. On the right side, the radial catalyst temperature profile was measured using thermocouples F, G, I and Z. Thermocouples labelled F, G and I were in the same relative positions as in the left-hand side, while thermocouple Z was in the insulation, approximately 8 cm outside of the reactor wall.

4. Results and discussion

In this section several experimental results are presented. As noted earlier, the first step in performing an experiment was to pre-heat the left side catalyst bed. Once the reactor was sufficiently pre-heated, an experiment could be performed. The temperature profiles for a typical experiment are shown in Fig. 4. This experiment was run for several hours with an inlet concentration of 0.22% CH_4. The superficial inlet velocity at inlet temperature (ambient, 23 °C) was 0.34 m/s, which is equivalent to a total mass flowrate of 50 kg/h. Each symmetric cycle was 600 s long. The axial temperature profiles recorded over 18 cycles are shown in Fig. 4. The profile was recorded at the end of each full cycle (that is, at the end of the reverse flow half cycle, with flow from left to right). Over the cycles, the overall temperature in the reactor increased. The shape of the centreline temperature profile shifts slightly over time and during a cycle, however, the reactor tends to accumulate thermal energy over time, as shown by the trend of increasing end-of-cycle temperature profile. The reactor was auto-thermal and self-sustaining under these conditions. Note that the dimensionless

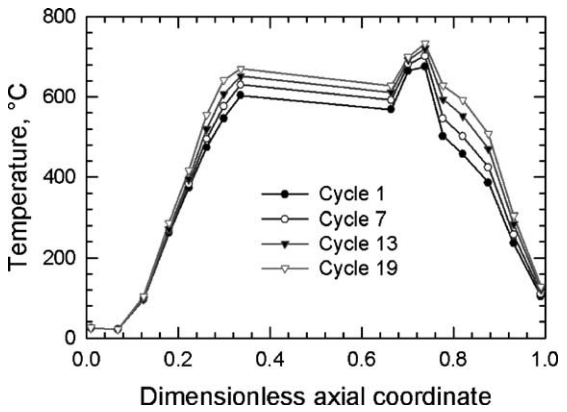

Fig. 4. Typical axial temperature profiles obtained during auto-thermal operation at 0.34 m/s inlet velocity and 0.22% methane. Cycles were 600 s in length. The profiles are shown at the end of the reverse flow half cycle, that is, with flow from the left section to the right section.

co-ordinate of 0.0 corresponds to the inlet of the left-hand side of the system. Therefore, the plot shows that the maximum temperature in the reactor occurred in the right-hand catalyst bed. The profiles shown in Fig. 4 were obtained after several hours of operation. In spite of this, the temperature is still increasing, indicating that heat is still accumulating in the reactor, and that the quasi-steady state was not attained. Indeed, because the reactor was well insulated, a quasi-steady state temperature was not achieved that was within the maximum tolerance of the reactor. In actual operation, the maximum temperature in the reactor would be controlled by the removal of energy from the central part of the reactor, although such operation was beyond the scope of the current investigation.

The effect of increased feed concentration is illustrated in Fig. 5. All conditions were the same as for those of Fig. 4, described above, however the inlet concentration of methane was 0.33% by volume for two of the shown profiles. Fig. 5 shows a comparison of the temperature profiles between the two runs. The profiles shown were obtained for a single cycle after quasi-steady state operation was obtained, and the profiles are shown at the end of the reverse flow and forward flow half cycles. There are a number of differences in the profiles, however, overall the experiment with higher methane concentration leads to higher reactor temperatures and faster temperature evolution, all other factors being equal. It can be seen that at the end of the forward flow half cycle the temperature rises in the left-hand reactor, although it does not reach the same value as the right-hand side at the end of the reverse flow half cycle. This effect is attributed to the presence of the electric pre-heater, which has the effect of adding thermal mass to the right-hand side. A word of caution, however, should be sounded about making detailed comparisons. For a proper comparison between different concentrations in a reactor, both systems must start at the same thermal state. Experimentally, it was exceptionally difficult to obtain the same initial thermal state at the beginning of a set of experiments, and the two experiments shown here did not start from exactly the same initial state. The thermal history of the reactor is very important.

One important feature observed in the reactor was the presence of radial temperature gradients. These gradients appear to be caused by the heat transfer processes involved during the transient operation. Two effects influence the results. The first is heat losses to the surroundings. The second is the thermal lag of the insulation and reactor walls, which are different from the reactor internals. These radial gradients are expected to affect the reactor performance.

The radial gradients were observed to change over time. This trend is illustrated in Figs. 6 and 7, which show the evolution of the observed radial gradients

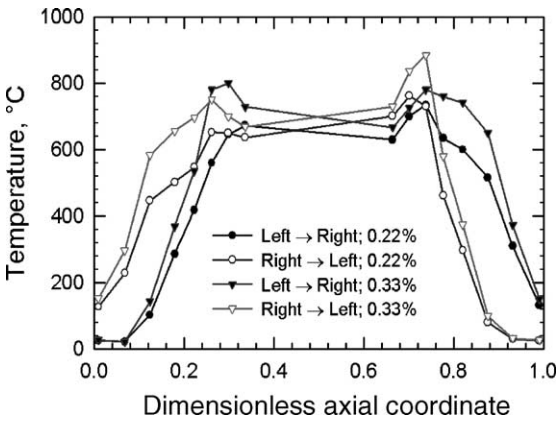

Fig. 5. Axial temperature profiles obtained for a single cycle at two different methane inlet concentrations and a common inlet velocity of 0.34 m/s. The symmetric cycles were 600 s long. For each case, the profile at the end of the forward flow (right to left) and reverse flow (left to right) half cycles are shown.

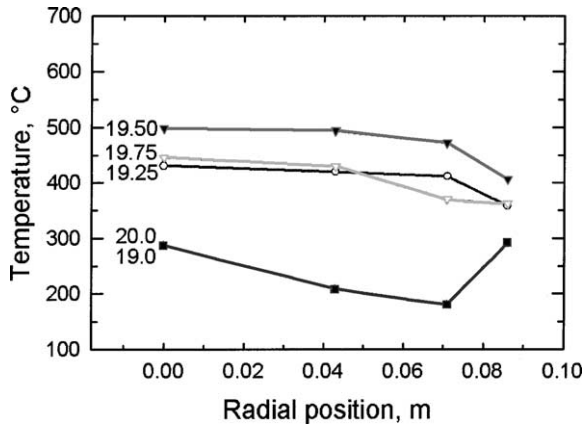

Fig. 6. Evolution of the radial temperature profile in the left side monolith inert section during a complete cycle. Inlet velocity was 0.34 m/s and methane concentration was 0.22%. Cycles were 600 s in length. Shown here is the monolith radial profile at different stages in a single cycle (with 19 designating the beginning of the cycle, 19.5 the end of the forward half cycle, and 20 being the completion of the cull cycle).

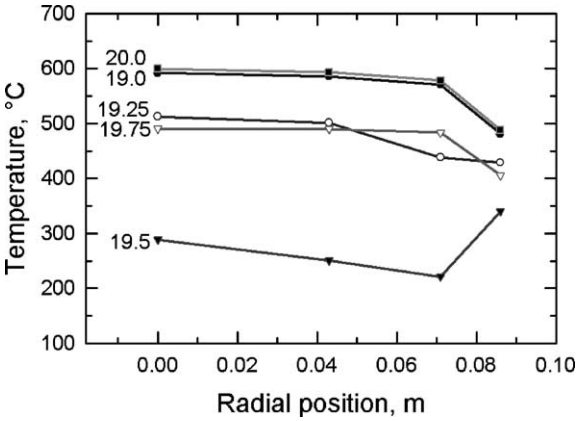

Fig. 7. Evolution of the radial temperature profile in the right side monolith inert section during a complete cycle. Inlet velocity was 0.34 m/s and methane concentration was 0.22%. Cycles were 600 s in length. Shown here is the monolith radial profile at different stages in a single cycle (with 19 designating the beginning of the cycle, 19.5 the end of the forward flow half cycle, and 20 being the completion of the full cycle).

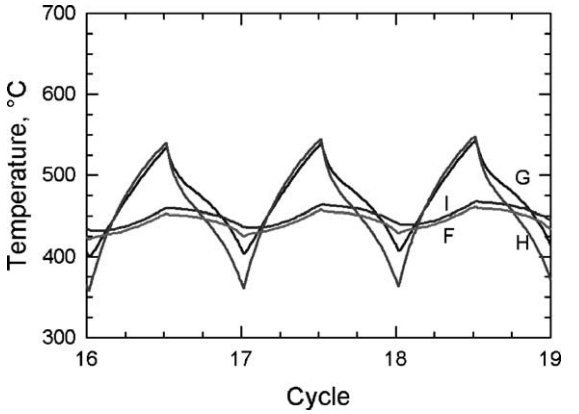

Fig. 8. Evolution of the temperatures in left side catalyst bed over the course of three cycles. Inlet velocity was 0.34 m/s (50 kg/h) and methane concentration was 0.22%. Cycles were 600 s long. The maximum temperature occurs at the mid-cycle point, which is the end of the forward flow half cycle.

in both inert monolith sections over the duration of a complete cycle. The cycle illustrated followed directly after cycle 19 shown in Fig. 4. The curve labelled 19 corresponds to the end of a reverse flow cycle, and therefore the left side monolith is at its lowest temperature. It is seen that the temperature initially falls as the radial co-ordinate increases, but then increases as the wall is approached. Then during the first half cycle (forward flow), the temperature in this section rises to a maximum (curve labelled 19.5, Fig. 4). Then, as the flow direction changes, the temperatures fall to essentially the same values as the beginning of the cycle. The cycling of the temperature illustrates the storage and subsequent release of thermal energy in the monolith section. The slower response of the thermocouple near the wall is attributed to the thermal mass of the wall and insulation, which responds more slowly than the reactor interior, owing both to a larger thermal mass and absence of convection.

The outlet monolith section typically has a similar profile shape, however, the behaviour is out of phase with the left-hand section. Thus, at the beginning of the experiment, which corresponded to the end of the previous reverse flow half cycle, the temperatures were at a maximum, with a decreasing trend in the radial direction. Then, as the forward flow cycle was begun, the monolith cooled until a minimum was reached at the mid-cycle point. Following the change in flow direction, the temperature returned to its previous value.

Significant radial gradients are also observed in the catalyst section. The temperature of the catalyst bed thermocouples with respect to time are shown in Fig. 8 for the left catalyst section and in Fig. 9 for the right catalyst section. The locations of the thermocouples

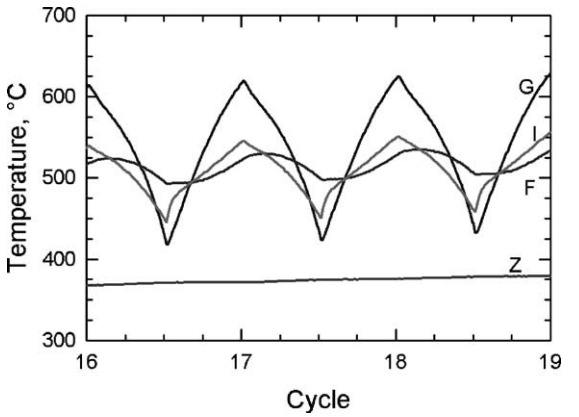

Fig. 9. Evolution of the temperatures in right side catalyst bed over the course of three cycles. Inlet velocity was 0.34 m/s (50 kg/h) and methane concentration was 0.22%. Cycles were 600 s long. The maximum temperature occurs at the end of the cycle, which is the end of the reverse flow half cycle. Note that thermocouple Z is in the reactor insulation.

are given in Fig. 3. In both graphs, thermocouple G (centreline) varies quite strongly, with a range of 200 °C for a cycle. Thermocouples F and I, which sit very near the reactor wall, may only change by 20–30 °C during a cycle. The difference between the centreline and the reactor wall temperature may be over 150 °C at specific times in the cycle.

The presence of radial gradients explains the shape of the centreline temperature profiles, and specifically the drop in temperature in the central part of the reactor. As shown by the radial profiles, the centreline temperatures are the highest. Therefore, when the gas exits the reaction section a mixing occurs between the gas at the high temperature (near the centre) and the gas at lower temperature (near the wall). The mixed gas has a lower temperature than the centreline.

The behaviour of the inner wall thermocouple H in the left-hand side is interesting in that it appears to behave much more like the centreline thermocouple than like the other wall thermocouples, I and F. These three thermocouples are all the same distance from the reactor wall, however, thermocouple H was located on the inside wall. Because the reactor is in the shape of a U with insulation packed in between, there is not the same potential for ambient losses in this area. Furthermore, the thermal characteristics of this section would also be different to an outside surface.

Because there were only two thermocouples inside the reactor in any direction from the centreline, a representative radial profile is difficult to obtain for the catalyst sections. We do not know the full shape of the profile at any given time step. However, from the centreline and the reactor wall temperatures, it is apparent that there is a strong (and ever-changing) radial gradient in the reactor. This gradient is important in considering the performance of the reactor under various conditions.

When the reactor was operated under conditions of relatively high methane concentration (0.89%) and relatively low superficial inlet velocity (0.21 m/s or 27.5 kg/h), the system exhibited behaviour that shall be referred to as dual peaks. Dual peaks, in this reactor configuration, were local hot spots in the catalyst sections. This phenomenon probably results from the ratio of the rates of heat generation by reaction to removal by convection. Once the reaction is initiated, the relatively high concentration of methane leads to faster generation, at a rate higher than can be redistributed through the catalyst bed and through the reactor. This operation is shown in Figs. 10 and 11. This type of local hot spot can become a problem. Unchecked temperature development may become a problem, leading to reactor or catalyst damage. Furthermore, these type of large hot spots can get trapped in the catalyst beds. When it is desired to operate the CFRR with heat removal between the beds, the heat extraction might become less efficient. Ideally, the hot spot should be passed through the central U-bend

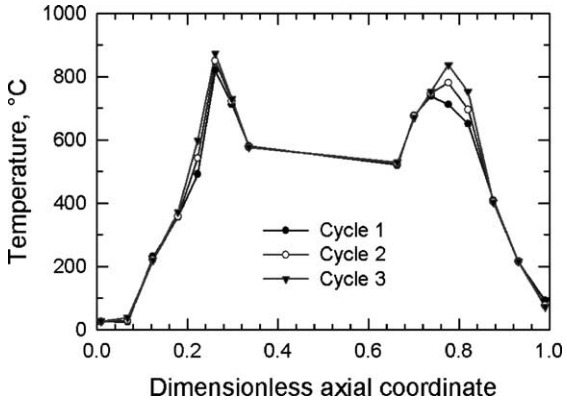

Fig. 10. Axial centreline temperature profiles for an experiment with high inlet methane concentration (0.89%) and relatively low inlet velocity (0.21 m/s). The formation of dual peaks was observed. The symmetric cycles were 400 s long. The profiles shown correspond tot he end of the reverse flow half cycle.

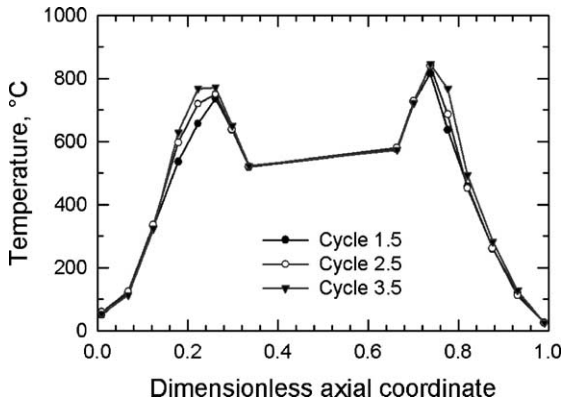

Fig. 11. Axial centreline temperature profiles for an experiment with high inlet methane concentration (0.89%) and relatively low inlet velocity (0.21 m/s). The formation of dual peaks was observed. The symmetric cycles were 400 s long. The profiles shown correspond to the end of the forward flow half cycle.

section. In both Figs. 10 and 11, the peak temperature is approximately 200–300 °C higher than the temperature in the open central section. As we see in Fig. 11, the peak temperature is approximately 900 °C, but the temperature of the gas in the open central section (where heat extraction takes place) is only 550 °C. The amount of thermal energy that may be extracted is dependent on the temperature of the gas in the open central section. Thermal energy extraction may not be as efficient if thermal energy is localised in the middle of the catalyst and not accessible to the heat exchanger. If the operational goal of this reactor in an application is as a utility energy source, then the temperature of the extracted heat/gas should be as high as possible.

Relatively high concentrations of methane are not necessarily bad for a CFRR (as long as the concentration is below the lower explosive limit), their use requires slightly different parameters when running the reactor. Increased heat extraction in the central section may significantly help in keeping the thermal energy from building up too much. Also, the localised peaks may be reduced by either increased conductive heat transfer (via increasing the superficial thermal conductivity of the catalyst packing) or increased convection heat transfer (via increasing the inlet flow rate). Alternatively, the length of the half cycles may be optimised to reduce energy localisation, but that is beyond the scope of this paper.

An experiment was performed to observe the response of the reactor to a sudden change in inlet concentration. The reactor was running with a superficial inlet velocity of 0.68 m/s (100 kg/h) at 0.33% methane. At the end of a forward flow half cycle the methane feed was cut off, however, the air flowrate was not changed. After a full cycle with 0% methane, the methane concentration in the feed was restored to 0.33%. The catalyst temperature profiles are shown in Figs. 12 and 13. Immediately following the feed cut off, the temperature in both catalyst sections began to drop. The drop was much more pronounced in the right-hand side reactor, with the highest recorded temperature dropping by almost 150 °C. A feed kill and restore cycle could potentially be used to test the stability and resilience of a reactor's thermal state. A reactor that is auto-thermal and stable should be able to recover from a one-cycle methane feed kill within a few cycles. The above reactor was able to do so approximately four cycles after the feed was restored. A reactor that is not auto-thermal will not survive the shock. However, a reactor that is just barely auto-thermal will most likely not survive a concentration shock. This may be a simple and fast test for a reactor's suitability to a practical application, but

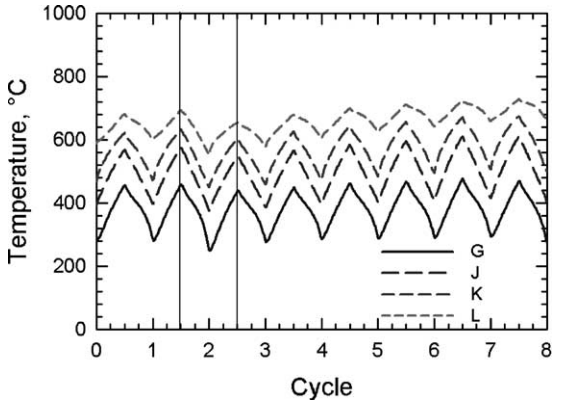

Fig. 12. Left-hand reactor catalyst centreline temperature response to a reactant feedout. The inlet velocity was 0.68 m/s with an inlet methane concentration of 0.33%. The cycles were 400 s long. The initial flow direction (at the point labelled cycle 0) was forward flow. At the mid-point of cycle 1, the methane feed was cut off (to 0%). All other inlet conditions remained the same. After one full cycle, the methane feed was restored to 0.33%.

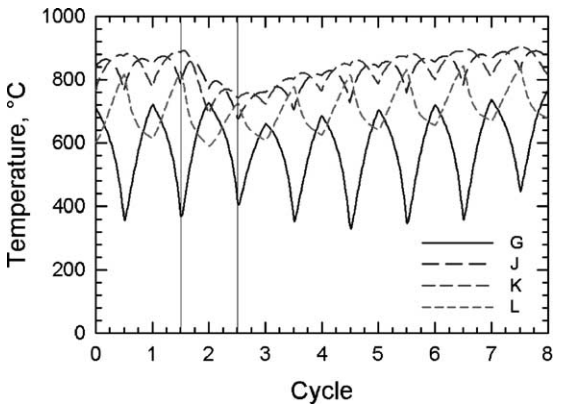

Fig. 13. Right-hand reactor centreline catalyst temperature response to a reactant feedout. The inlet velocity was 0.68 m/s with an inlet methane concentration of 0.33%. The cycles were 400 s long. The initial flow direction (at the point labelled cycle 0) was forward flow. At the mid-point of cycle 1, the methane feed was cut off (to 0%). All other inlet conditions remained the same. After one full cycle, the methane feed was restored to 0.33%.

it does not discriminate between a self-extinguishing thermal state and a borderline thermal state. Distinguishing between those two states may require simply letting the reactor run for an extended period to see if it eventually extinguishes or not. This process may take many hours to show a definite trend. Variations on this test could include placing the shock at different points in the cycle, lengthening the shock to more cycles, or lowering instead of killing the methane feed.

5. Conclusions

Based on the experiments performed on the CFRR a number of conclusions were drawn. The first is that it is possible to maintain auto-thermal operation of the reactor at methane concentrations as low as 0.22% with feed at ambient temperature. This operation would not be possible in a direct flow system. The overall performance of the system is dependent on methane concentration, cycle time and velocity.

The experimental results indicate the presence of radial gradients in the reactor. These gradients are expected to affect reactor performance, and must be considered when evaluating the dynamics of the reactor. A traditional centreline temperature profile is insufficient to capture the dynamics of the system adequately. The gradients are dynamic and complex, and appear to be influenced by several competing factors.

In a system with relatively low inlet velocity and relatively high methane concentration, there is a chance of creating localised hot spots in the catalyst. These hot spots form when the thermal energy generated by the reaction is not fully distributed through the catalyst. Increasing the heat transfer between hot spots and the rest of the catalyst by increasing the effective thermal conductivity of the catalyst or by increasing convection heat transfer may help to delocalise the thermal energy. A large disparity between the peak temperature and the extraction temperature will lower efficiency of energy extraction.

A reverse flow catalytic converter is a very dynamic system. To fully understand all of the processes in the system, more research must be done. While much of the future work must be experimental, there is a tremendous scope for computer aided design in this process. This latter aspect is predicated on the development of a robust simulator that can adequately capture the dynamics of the system. The description of such a simulator will be the focus of a future paper.

Acknowledgements

Partial financial support for this work was provided by the Natural Sciences and Engineering Research Council of Canada.

References

[1] R.E. Hayes, S.T. Kolaczkowski, Introduction to Catalytic Combustion, Gordon and Breach, Reading, UK, 1997.
[2] G. Veser, J. Frauhammer, Modelling steady state and ignition during catalytic methane oxidation in a monolith reactor, Chem. Eng. Sci. 55 (2000) 2271–2286.
[3] B. Liu, M.D. Checkel, R.E. Hayes, Experimental study of a reverse flow catalytic converter for a dual fuel engine, Can. J. Chem. Eng. 79 (2001) 491–506.
[4] W. Ye, Catalytic oxidation of methane over supported palladium catalysts, M.Sc. Thesis, University of Alberta, Edmonton, 1999.
[5] R.E. Hayes, S.T. Kolaczkowski, P.K.C. Li, S. Awdry, The palladium catalysed oxidation of methane: reaction kinetics and the effect of diffusion barriers, Chem. Eng. Sci. 56 (2001) 4815–4835.
[6] C.F. Cullis, D.E. Keene, D.L. Trimm, Pulse flow reactor studies of the oxidation of methane over palladium catalysts, J. Chem. Soc., Faraday Trans. 67 (1971) 864–876.
[7] P. Forzatti, G. Groppi, Catalytic combustion for the production of energy, Catal. Today 54 (1999) 165–180.
[8] C. Sapoundjiev, J. Chaouki, C. Guy, D. Klvana, Catalytic combustion of natural gas in a fixed bed reactor with flow reversal, Chem. Eng. Commun. 125 (1993) 171–186.
[9] S. Cimino, A. Di Benedetto, R. Pirone, G. Russo, Transient behaviour of perovskite-based monolithic reactors in the catalytic combustion of methane, Catal. Today 69 (2001) 95–103.
[10] D.A. Frank-Kamenetski, Diffusion and Heat Exchange in Chemical Kinetics, Princeton University Press, Princeton, NJ, 1955.
[11] Y.S. Matros, G.A. Bunimovich, Reverse-flow operation in fixed bed catalytic reactors, Catal. Rev. 38 (1996) 1–68.
[12] B. Liu, R.E. Hayes, M.D. Checkel, M. Zheng, E. Mirosh, Reversing flow catalytic converter for a natural gas/diesel dual fuel engine, Chem. Eng. Sci. 56 (2001) 2641–2658.
[13] V.O. Strots, G.A. Bunimovich, Yu.Sh. Matros, M. Zheng, E.A. Mirosh, Advanced catalytic converter system for natural

gas powered diesel engines, Stud. Surf. Sci. Catal. 119 (1998) 907–912.
[14] K. Hanamura, R. Echigo, S.A. Zhdanok, Superadiabatic combustion in a porous medium, Int. J. Heat Mass Transfer 36 (1993) 3201–3209.
[15] B. Liu, A study of reverse flow catalytic converters, Ph.D. Thesis, University of Alberta, Edmonton, 2000.
[16] G. Grozev, C.G. Sapoundjiev, Modelling of the reversed flow fixed bed reactor for catalytic decontamination of waste gases, Chem. Eng. Technol. 20 (1997) 378–383.
[17] A.J. Rankin, R.E. Hayes, S.T. Kolaczkowski, Annular flow in a catalytic monolith reactor: the significance of centreline probe temperatures engineering research and design, Trans. I Chem. E, Part A 73 (1995) 110–121.